International Journal of Advanced Research in Engineering Technology & Science
ISSN: 2349-2819
Email: editor@ijarets.org Volume-7, Issue-1 January- 2020 www.ijarets.org

SYNTHESIS OF CYCLOHEXADIENONE CORED CABAZOLE DENDRIMERS WITH TRIAZOLE BRIDGING UNIT

Dr. Uday Kumar

Associate Professor , Department of Chemistry

Jamuni Lal College,Hajipur.

(B.R.A.Bihar University, Muzaffarpur.)

ABSTRACT

By using convergent synthesis and click chemistry, (S)-BINOL cored dendrimers 1–3 with a rhodamine B surface group and a triazole bridging unit were successfully synthesized up to the second generation in good yield. The chiro-optical property of the synthesized dendrimers demonstrates that the specific rotation rises as the order of dendrimer grows from the zeroth -generation dendrimer to the second -generation dendrimer. This was discovered by comparing the specific rotation of the first- generation dendrimer to the second-generation dendrimer. In cyclic voltammetry, the electrochemical characteristics of dendrimers 1, 2, and 3 displayed behavior that was quasi-reversible. It was discovered that the anticancer activity of the dendrimer 3 of the second generation against human hepatocellular carcinoma cells was superior to that of the dendrimers 1 and 2 of the lower generation.

keywords: *cyclohexadienone cored, triazole bridging*

INTRODUCTION

Chiral dendrimers are fundamentally unlike to achiral dendrimers because chiral dendrimers have distinct features that are derived from their well-defined and well-regulated stereospecific structures. Chiral dendrimers, thanks to the one-of-a-kind chiro-optical characteristics they possess, are able to accomplish significant goals, and as a result, they have a broad variety of applications in the fields of chemistry, biology, and technology. As a consequence of this, the synthesis of chiral dendrimers has garnered a lot of interest and developed into a bustling area of research. A significant amount of work has been done over the course of the past two decades in the area of the synthesis of a broad range of functionalized dendrimers. These dendrimers have distinctive properties that may be utilized for a variety of applications in a variety of domains, including catalysis, biology, and technology.

Chirality is a property that is present in a great number of biological systems and plays a significant part in the dynamic between structure and function. The synthesis of big compounds that exhibit chirality provides organic chemists with not just a synthetic challenge but also access to a broad range of novel molecules. There is a family of chemicals known as chiral dendrimers that provide the opportunity to examine the effect that chirality has on macromolecular systems. Both the effect of chiral units on supramolecular structures and the implementation of such structures in fields such as catalysis, biosensor research, and optical device design provide a significant amount of difficulty. In order to get an in-depth comprehension of the chiro-optical characteristics, it is necessary to have well-defined polymers that have an accurate molecular weight and polydispersity. In this regard, dendrimers are great candidates for such applications due to the fact that their structure, topology, and molecular weight are all very well characterized.

Chiral dendrimers are an essential component for the development of highly sensitive macromolecular conformational structures that operate as a result of supramolecular interactions. Chiral dendrimers have the potential to be used in a wide range of applications, including but not limited to drug administration, catalysis (including enantioselective catalysis), as catalyst supports, phase transfer catalysts, and membrane reactors, amongst other things. (S)-BINOL cored dendrimers exhibit a variety of biological actions, including those that are antibacterial, anti-inflammatory, antimicrobial, and anticancer.14 Therefore, the (S)-BINOL unit plays a significant role in both the field of liquid crystals and the field of biology.15 Dendrimers that include a (S)-BINOL core can be employed as entiaselective Lewis acid catalysts, in addition to exhibiting unique chiro-optical and photophysical characteristics.16 These qualities can be found in dendrimers.17 In chemical synthesis, chiral dendrimers containing the (S)-BINOL core can function both as chiral bases and as chiral auxiliaries.18 In addition, as the number of dendrimer generations increases, the distance between the dendritic wedges grows, which has the potential to increase the dihedral angle at the naphthyl unit. This transforms the dendrimers into chiral auxiliaries with a greater value of molar rotation. In this paper, we disclose a flexible and extremely effective method for the synthesis of the (S)-BINOL cored dendrimers 1 to 3, as well as their chiro-optical, electrochemical, and anticancer activities (Fig. 1).

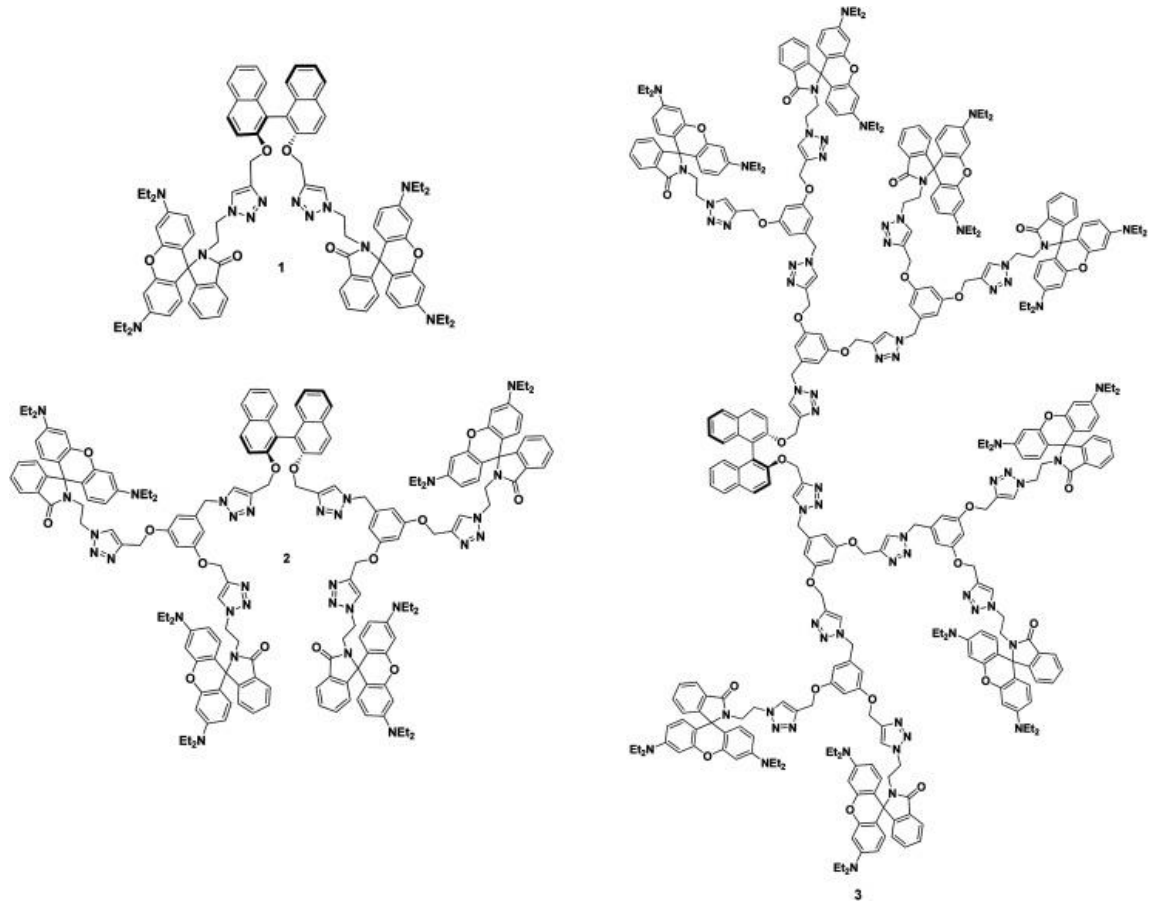

Fig. 1 shows the molecular structure of chiral dendrimers 1, 2, and 3 with (S)-BINOL cores and rhodamine B decorations.

RESEARCH METHODOLOGY

Cell line and cell culture

We obtained the human hepatocellular carcinoma cell line (Huh-7) from the National center for cell sciences (NCCS), which is located in Pune. Huh-7 cells were grown in T-25 culture flasks and 30 mm Petri dishes containing Dulbecco's Modified Eagle Medium (DMEM) with 4.5 g L1 glucose and L-glutamine (Lonza, USA). This medium was also supplemented with 10% fetal bovine serum (HI media) and 1% of antibiotics (100 U mL1 penicillin, 100 g mL1 of streptomycin, and 0.

Cytotoxicity study by MTT assay

A 96-well tissue culture plate was seeded with about 3 x 103 cells per well, and the cells were allowed to proliferate for the duration of the experiment. After the cells had reached 80% confluency, the media was discarded, and they were subjected to a variety of concentrations of rhodamine B, dendrimer 1, 2, and 3 over a period of twenty-four hours. The concentrations ranged from 5–100 M. Following the incubation time, 10 L of MTT (5 mg mL1) was added, and the mixture was put back into the incubator for another 4 hours at 37 degrees Celsius in the dark. After 30 minutes of stirring with 50 L of DMSO, the purple-colored formazan crystal that had developed at the bottom was dissolved. The absorbance was measured on the microplate reader at a wavelength of 570 nm. A560 nm of treated cells divided by A560 nm of control cells multiplied by 100 gives a percentage of cell viability.

Morphological study by a phase-contrast microscope

On top of cover slips, cells were sown into tissue culture plates with six wells. After an initial period of 24 hours, the medium was discarded, and the cells were then subjected to a treatment with rhodamine B dendrimers 1, 2, and 3, followed by an additional period of 24 hours of incubation. After the incubation period, the cells were fixed by adding 400 L of 4% formaldehyde in PBS for 20 minutes at room temperature. The cells were then rinsed twice with PBS for 5 minutes each time. After the cells had been fixed, they were given two washes with ice-cold PBS. After carefully mounting the cover slips on the glass slide, the cell morphology was examined using a phase contrast microscope and photographed (with a Nikon microscope ECLIPSE 400, Japan) at a magnification of 10 times using the Nikon microscope.

RESULT AND DISCUSSION

A stepwise synthesis process was utilized in order to produce (S)-BINOL cored rhodamine B adorned triazole bridging dendrimers 1, 2, and 3. In order to obtain the desired chiral triazolyl dendrimers, the processes of propargylation, agitation, and click reactions were utilized. In order to make the (S)-BINOL cored rhodamine B adorned dendrimers 1, 2, and 3, a convergent synthetic approach was used to make the rhodamine B-capped azido dendrons 6, 9, and 11. This resulted in good yields of the synthesized compounds. In order to explore the utility of rhodamine B as a surface unit in dendrimers, the dendritic wedge 6 was synthesized, as outlined in Scheme 1. The precursor 4 of rhodamine B was refluxed in $POCl_3$ for 18 h and concentrated by evaporation, and the rhodamine B acid chloride thus obtained was dissolved in CH_3CN. 2-Bromoethylamine hydrobromide was subsequently added in the presence of triethylamine and stirred at room temperature for 24 h under N_2 atmosphere to afford the rhodamine B dendritic bromide 5, which was further reacted with NaN_3 in a mixture of acetone: water (4: 1) at 60 °C to yield the rhodamine B azido dendron 6 [19] in 95% yield (Scheme 1).

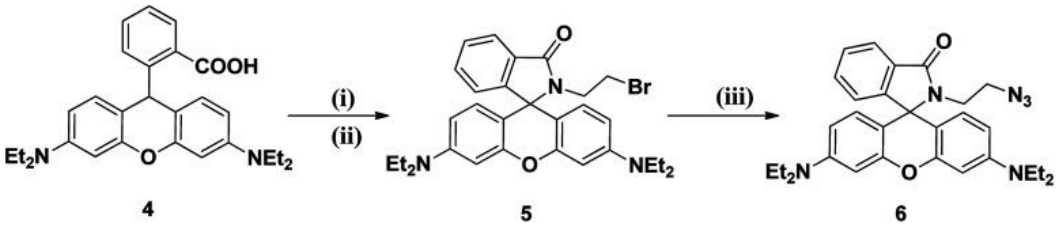

Scheme 1: POCl3, 110 °C, 18 hours, and 2-bromoethyl amine, CH3CN, TEA, rt, 24 hours, 5 (64%). NaN3, acetone, and water (4:1) at 60 °C for 10 hours and 6 (95%).

We then focused our attention on the synthesis of precursors for the first and the second- generation dendrimers 2 and 3. The synthesis of the first -generation dendritic aside 9 is shown in Scheme 2. The reaction of 3,5-bis(propargyl)benzyl chloride 7 with 2.1 equiv. of rhodamine B azido dendron 6 under Cu(I)-catalyzed click reaction conditions afforded the first- generation dendritic chloride 8 in 92% yield, which on further treatment with NaN_3 in a mixture of acetone/water (4: 1) at 60 °C for 10 h gave the dendritic aside 9 [19] in 94% yield (Scheme 2). Then, we focused on the synthesis of the second- generation dendritic aside 11 from the first generation dendritic aside 9. The reaction of 1.0 equiv. of 3,5-bis(propargyl)benzyl chloride 7 with 2.1 equiv. of the azido dendron 9 under click reaction conditions *viz.*, $CuSO_4 \cdot 5H_2O$ and sodium ascorbate in a 1: 1 mixture of THF and water at room temperature afforded the second -generation dendritic chloride 10 in 86% yield, which on further treatment with NaN_3 in a mixture of acetone/water (4: 1) gave the dendritic aside 11 in 92% yield (Scheme 2).

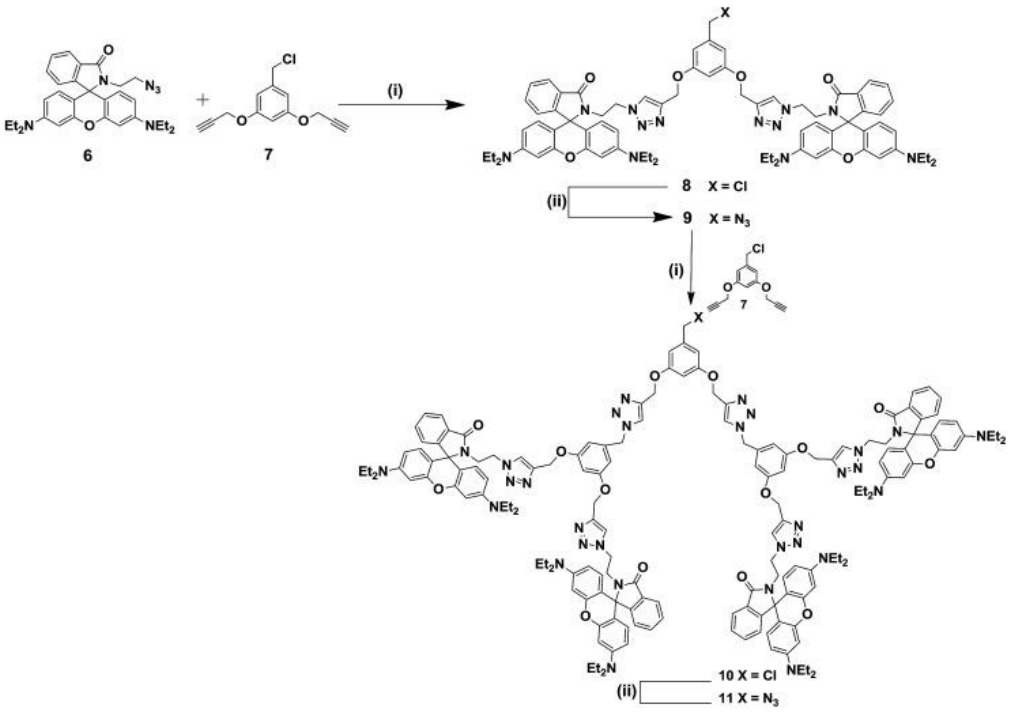

Reagents and conditions in Scheme 2: CuSO45H2O (5 mol%), sodium ascorbate (10 mol%), THF-H2O (1:1), 10 h, 8 (92%), and 10 (86%), respectively. (ii) NaN3, acetone: water (4:1), 60 °C, 10 hours, 9 (94%), and 11 (92%).

From the spectroscopic and analytical data, the structure of the dendritic aside and chloride 8 was identified. The second- generation dendritic chloride 10's 1H NMR spectrum showed two triplets at 3.59 and 4.16 ppm for the rhodamine N-methylene and triazolyl N-methylene protons, as well as three singlets at 4.68, 5.03, and 5.40 ppm for the chloro methyl, O-methylene, and inner triazolyl N-methylene protons, respectively. Additionally, the triazole protons showed up as the rhodamine N-methylene and triazolyl N-methylene carbons were visible in the 13C NMR spectra of substance 10 at 47.8 and 48.2 ppm, respectively, as well as signals for the inner triazolyl N-methylene, chloro methyl, and O-methylene carbons at 52.0, 62.9, and 64.2 ppm, respectively. Along with the other aliphatic and aromatic carbon signals, the triazole carbon signal was detected at 152.4 ppm and the rhodamine B carbonyl signal was detected at 168.3 ppm. Similar to this, the 1H and 13C spectral and analytical data verified the structure of the azido dendron 11.The (S)-BINOL cored rhodamine B decorated dendrimers 1, 2 and 3 were synthesized regioselectivity in 87%, 86% and 78% yields, respectively, by the reaction of 1.0 equiv. of the bispropargyloxy (S)-BINOL core unit 12 [20] with 2.1 equiv. of each of the dendritic asides 6, 9 and 11 in the presence of $CuSO_4 \cdot 5H_2O$, sodium ascorbate in a mixture of THF and water (1 : 1) at room temperature for 12 h, as shown in Scheme 3.

Chiro-optical property of (S)-BINOL cored rhodamine B decorated dendrimers 1–3

For the (S)-BINOL cored chiral dendrimers 1, 2, and 3, the specific rotation and molar specific rotation values were measured at 589 nm in DCM at a concentration of 1 103 M. Table 1 provides the particular rotation []25D and molar rotation values. Because the dendrimers 1, 2, and 3 contain the (S)-BINOL core unit, they can function as chiral auxiliary molecules. From the first- generation dendrimer (G0) to the second -generation dendrimer (G2), the negative specific rotation value decreases with dendrimer generation. (S)-BINOL has a rotational value of 35.5. The zeroth, first, and second- generation dendrimers, respectively, have specific rotation values of 18.4, 13.5, and 4.1. Due to the intramolecular repulsion of the bulky dendritic wedges, the dihedral angle at the (S)-BINOL unit likewise increases with the density of the wedges. To reduce the steric repulsion between the dendritic wedges and lower the negative value of the specific rotation, which may move closer to the positive side, the dihedral angle at the (S)-BINOL core increases as the formation of the dendrimer grows. The molar rotation value for the zeroth- generation dendrimer 1 (G0), the first- generation dendrimer 2 (G2), and the second -generation dendrimer 3 (G2) in this study was determined to be 132.3, 161.2, and 202.7, respectively. The dendrimers 1, 2, and 3 were found to have molar rotation values of 132.2, 161.2, and 202.7, respectively, as a result of an increase in molecular mass.

Specific and molar rotational values of (S)-BINOL cored dendrimers 1, 2 and 3

Dendrimers	Calculated mass	Specific rotation $[\alpha]^{25}_D$	Molar rotation
1 (G0)	1383	−18.4	−132.2
2 (G1)	2885	−13.5	−161.2
3 (G2)	5893	−4.1	−202.7

Circular dichroism spectral studies

At a concentration of 1.0 M in DCM as the solvent, the circular dichroism spectra of the zeroth- generation dendrimer 1 (G0), the first- generation dendrimer 2 (G2), and the second -generation dendrimer 3 (G2) were obtained (Fig. 2). The absorbance values are shown in Table 2. A negative peak and a positive peak were visible in the (S)-BINOL's circular dichroism spectra at 330 and 342 nm, respectively. The zeroth generation 1 (G0) displayed a negative peak with an absorbance intensity of 6.34 M1 cm1 at 329 nm and a positive signal with an absorbance intensity of +1.10 M1 cm1 at 342 nm. The first- generation dendrimer 2 (G1) had two peaks: a negative peak with an absorbance intensity of 17.41 M cm-1 at 330 nm and a positive peak with an absorbance intensity of +8.90 M cm-1 at +8.90 nm. Similar to the first-generation dendrimer (G1), the second -generation dendrimer (G2) had a negative peak at 330 nm with an absorbance intensity of 10.43. However, compared to the zeroth- generation dendrimer 1 (G0) and the first- generation dendrimer 2 (G1), the positive peak signal at 342 nm had the highest intensity of +22.14 M1 cm1, which indicates that the dihedral angle at the (S)-BINOL unit increases and causes the highest absorbance intensity of the positive signal. As a result, when large dendritic wedges are joined, the circular dichroism spectrum also reveals an increase in the dihedral angle at the (S)-BINOL unit.

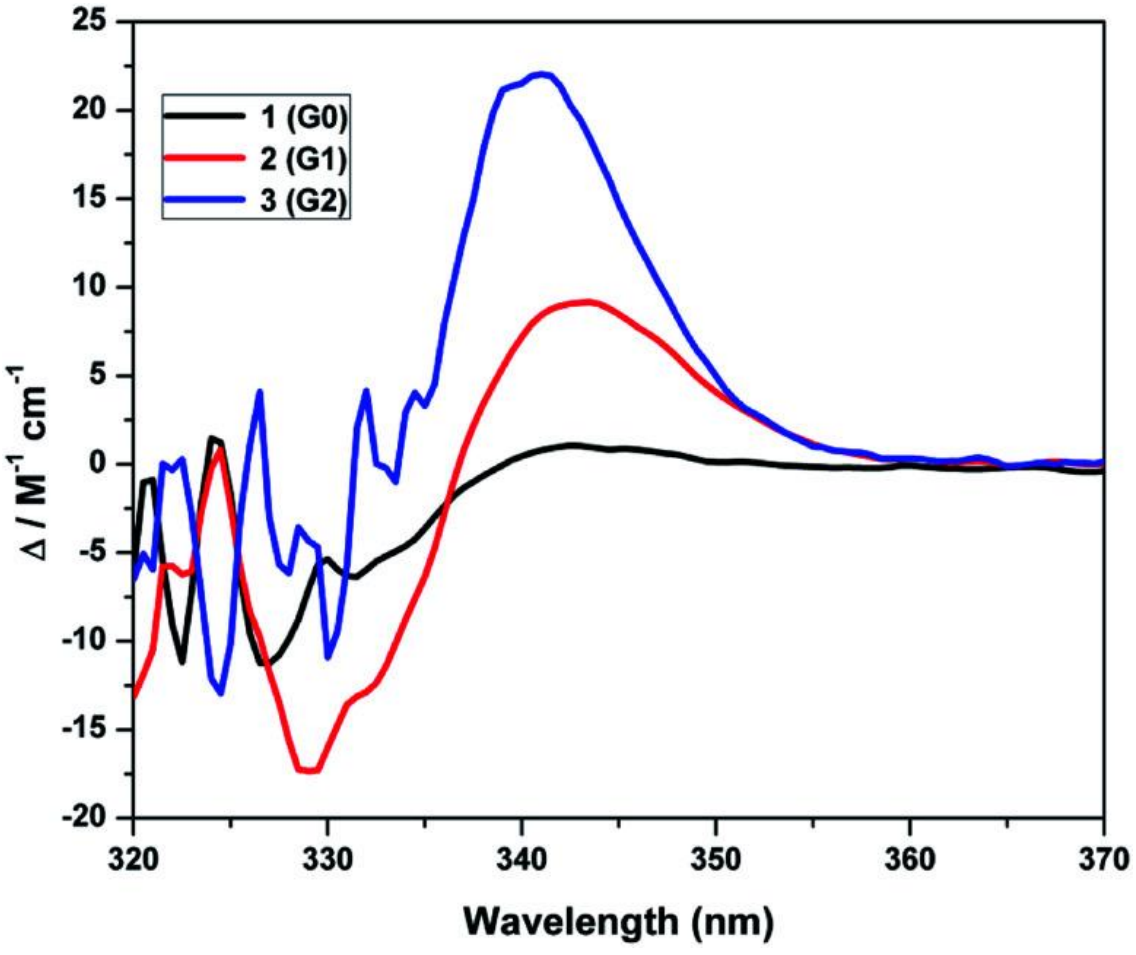

Fig. 2 Circular dichroism spectra of dendrimers 1-3 in DCM at room temperature at a concentration of 1.0 M.

Circular dichroism spectrum data of (S)-BINOL, the 0th 1, the 1st 2, and the 2nd generation dendrimers (G0, G1, and G2, respectively)

Dendrimers		Absorbance intensity (nm)	Negative peak (M^{-1} cm^{-1})	Absorbance intensity (nm)	Positive peak (M^{-1} cm^{-1})
1 (G0)		329	−6.34	342	+1.10
2 (G1)		330	−17.41	342	+8.92
3 (G2)		330	−10.43	342	+22.14

Photophysical property of (S)-BINOL cored rhodamine B decorated dendrimers 1–3

The dendrimers 1, 2, and 3's emission and absorption spectra were captured in DCM at room temperature. The absorbance spectra of dendrimers 1, 2, and 3 are depicted in Fig. 3a, and Table 3 provides a summary of the absorption values. The three main absorption bands for dendrimer 1, 2, and 3 were located between 478 and 486, 515 and 517, and 554-555 nm, respectively (Fig. 3). The rhodamine B unit's absorption band is often found between the wavelengths of 540 and 560 nm. The absorbance bands at 515-517 and 554-535 nm may be caused by the n-* transitions from the (S)-BINOL and rhodamine B units, respectively. The absorbance band at 478-486 nm may be caused by -* transitions. From the first generation of dendrimers to the second generation, the intensity of the absorption rises. There are just two rhodamine B units in the zeroth-generation dendrimer. However, the first- and second-generation dendrimers, respectively, include 4 and 8 rhodamine B units. when a result, the strength of the absorbance band presumably increases when one moves from the first to the second generation as a result of the increase in the number of rhodamine B surface group from 4 to 8 units.

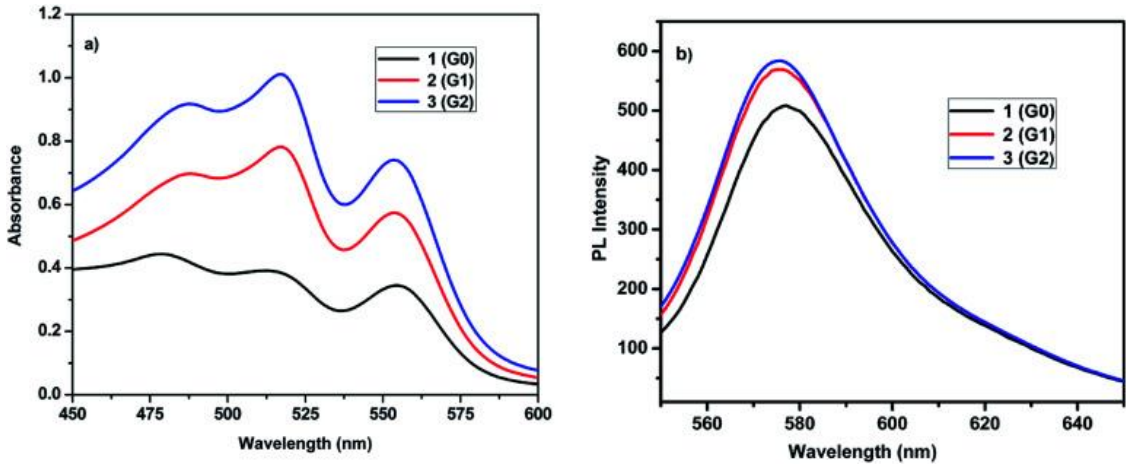

Figure 3 shows the emission and absorbance spectra of dendrimers 1-3 at a concentration of 1 103 M in room-temperature DCM.

The electrochemical parameters, fluorescence data, and absorption for the rhodamine B-decorated dendrimers 1, 2, and 3 in DCM (1 105 M)

Dendrimers	**λ_{abs} max (nm)**	**Absorption extension coefficient ($\varepsilon \times 10^{-5}$) M^{-1} cm^{-1}**	**λ_{em} max (nm)**	**ϕ_F**	**E_{pc}**	**E_{pa}**	**$\Delta E = E_{pc} - E_{pa}$**
1 (G0)	478, 515, 555	0.44, 0.39, 0.34	576	0.79	−0.42	+0.87	0.45
2 (G1)	486, 517, 554	0.69, 0.78, 0.57	575	0.73	−0.46	+0.85	0.39
3 (G2)	486, 517, 554	0.96, 1.00, 0.74	575	0.64	−0.41	+0.91	0.50

The emission spectra of the (S)-BINOL cored dendrimers 1, 2, and 3 in DCM are shown in Fig. 3b, and Table 3 contains the fluorescence characteristics. On stimulation at 520 nm, all of the dendrimers displayed strong florescence emission peaks between 575 and 576 nm. The valency effect is a concept in dendrimer chemistry that describes how, as the number of rhodamine B surface groups rose, so did the relative strength of the emission band from the zero, first, and second-generation dendrimers.21 Using quinine sulphate as the reference, the fluorescence quantum yield (F) of dendrimers 1-3 was calculated in DCM. Table 3 is a list of the dendrimers 1-3's quantum yields. The quantum yield continually declines with increasing generation. In comparison to the lower generation dendrimers 2 (G1) and 1 (G0), the second-generation dendrimer 3 (G2) effectively quenches fluorescence due to its larger concentration of rhodamine B units. The quantum yield drops to 0.64 as fluorescence quenching becomes more effective in the second-generationdendrimer.

Electrochemical studies of (S)-BINOL cored rhodamine B decorated dendrimers 1–3

Cyclic voltammetry (CV) was used to examine the redox behavior of dendrimers 1, 2, and 3 at room temperature with a scan rate of 50 mV s1. As the working electrode, Pt wire served as the counter electrode, while Ag/AgCl served as the reference electrode. The supporting electrolyte used in the CV investigations was tetrabutylammonium perchlorate (0.1 M), which was dissolved in solutions of the substrates (1 mM) in CH2Cl2. In the cyclic voltammogram test, all of the as-synthesized dendrimers displayed electrochemical responses. The cyclic voltammograms of dendrimers 1, 2, and 3 are shown in Fig. 4, and the electrochemical characteristics are reported in Table 3.

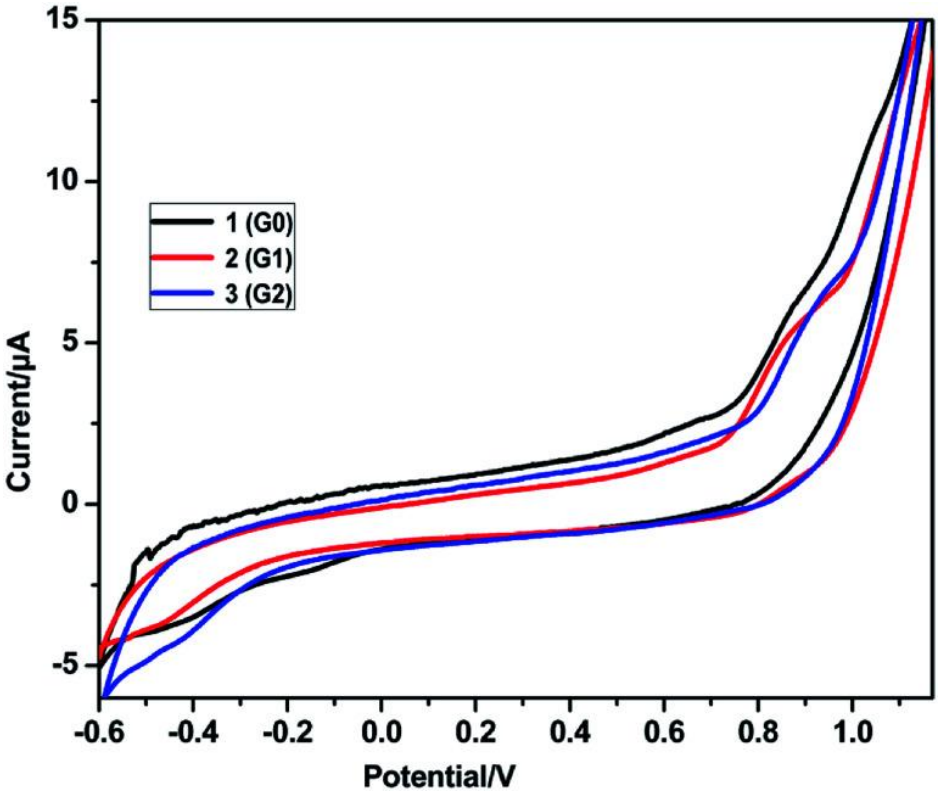

Fig. 4: Scannable at 50 mV per second, cyclic voltammogram of dendrimers 1-3 in CH2Cl2 (1 10-3 mol L1).

All of the dendrimers 1, 2, and 3 coated with rhodamine B had oxidation and reduction potentials that ranged from 0.6 to +1.2 V. Rhodamine B decorated dendrimers 1, 2, and 3 were discovered to have reversible oxidation potentials of 0.42, 0.46, and 0.41 V, respectively, while reversible reduction peaks were detected at +0.87, +0.85, and +0.91 V, respectively. More triazole units, which are responsible for the oxidation peak, are present when potential values are negative. Due to the prolonged conjugation of the aromatic rhodamine B moiety's higher energy need during the reduction process, all dendrimers had a high positive potential range of +0.85 to +0.91 V. Thus, in cyclic voltammetry, all dendrimers 1 to 3 had almost reversible behavior as they were produced.

Anti-cancer activity of (S)-BINOL cored rhodamine B decorated dendrimers 1–3

Using the MTT assay, the cytotoxicity of all the produced rhodamine B dendrimers 1, 2, and 3 was evaluated against the HUH-7 human hepatocellular carcinoma cell line. According to this study, the viability of HUH-7 cells reduced when dendrimer concentrations rose. The findings are shown in Table 4 and Figs. 5-8. The ability of the rhodamine B dendrimers to suppress the development of the HUH-7 hepatocellular cancer cell line was assessed. The findings demonstrate that rhodamine B dendrimers limit the proliferation of cancer cells, and it was shown that this effect increases as dendritic production increases. The rhodamine B unit's increased anticancer action was caused by the nitrogen and oxygen atoms. Rhodamine B dendrimer 3 (G2) was discovered to have an IC50 value of 15 M, while dendrimers from lower generations 2 (G1) and 1 (G0) had IC50 values of 20 M and 25 M, respectively. The higher generation dendrimers clearly exhibit better inhibition of the growth of cancer cells than the lower generation dendrimers, as shown by the IC50 values. This could be because the higher generation dendrimers aggregate to a greater degree, as demonstrated by the

absorbance and fluorescence studies. Due to the aggregation effect, as shown by the photophysical characteristics, the higher generation rhodamine B dendrimer suppresses the proliferation of cancer cells to a larger extent than the lower generation dendrimers 1 (G0) and 2 (G1). The higher generation dendrimer 3 (G2) among the three dendrimers suppresses the proliferation of cancer cells more effectively than the lower generation dendrimers 1 (G0) and 2 (G1). Table 4 displays the inhibitory activity of the three dendrimers.

Inhibition of the cell viability IC_{50} value under different concentrations of 5 µM, 10 µM, 15 µM, 20 µM, 25 µM, 50 µM and 100 µM dendrimers 1 (G0), 2 (G1) and 3 (G2) against the growth of the human hepatocellular carcinoma cell line (HUH-7)[a]

Different concentrations of rhodamine B dendrimers 1, 2, 3	**Percentage of cell viability (%)**		
	1 (G0)	**2 (G1)**	**3 (G2)**
Control	100 ± 0	100 ± 0	100 ± 0
5 µM	93.9 ± 2.8	88.9 ± 2.6	73.9 ± 2.1
10 µM	82.0 ± 2.4	77.0 ± 2.3	61.1 ± 1.7
15 µM	75.9 ± 2.2	60.9 ± 1.8	50.3 ± 1.5
20 µM	63.0 ± 1.8	50.8 ± 1.9	41.9 ± 1.2
25 µM	50.8 ± 1.4	44.8 ± 1.4	34.9 ± 1.0
50 µM	42.9 ± 1.2	32.9 ± 0.9	22.1 ± 0.8
100 µM	31.8 ± 0.8	23.6 ± 0.4	17.0 ± 0.5
IC_{50} value	25 µM	20 µM	15 µM

Value expressions are used.Values are stated in terms of Mean and SEM. Mean values are triple-checked in the Mean SEM. Mean values are triple-checked.

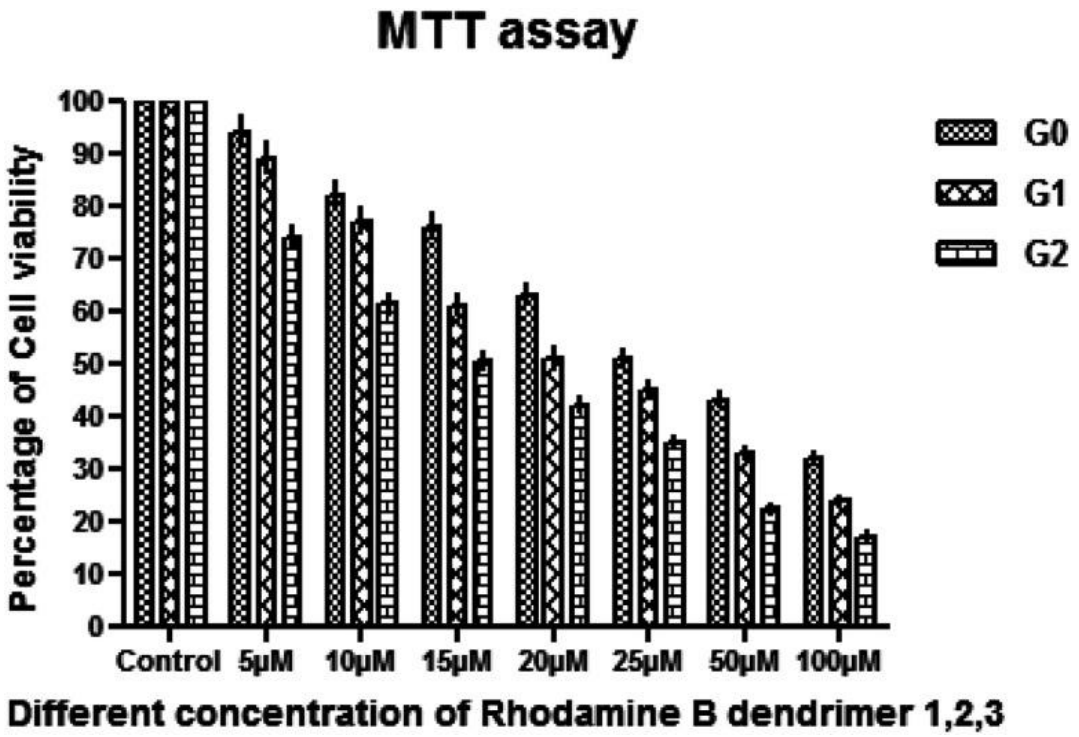

Fig. 5 shows anticancer activity of dendrimers 1 (G0), 2 (G1), and 3 (G2) against the HUH-7 human hepatocellular carcinoma cell line at various doses.

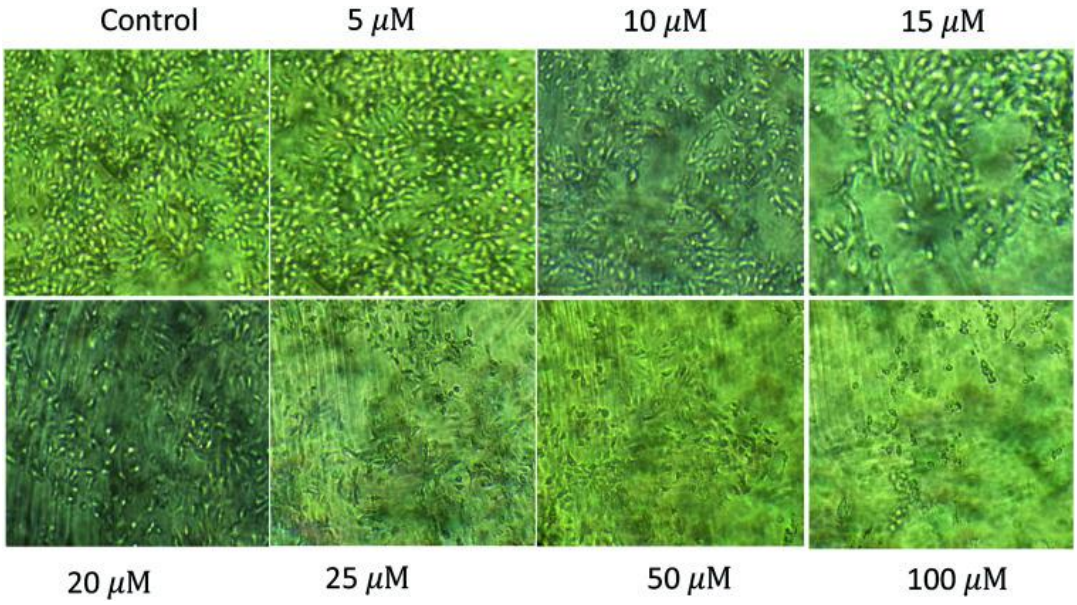

Figure 6 illustrates the zeroth-generation dendrimer 1 (G0)'s cytotoxicity on the HUH-7 human hepatocellular carcinoma cell line and its 50 M IC50.

CONCLUSION

Through the use of a click reaction, (S)-BINOL cored, rhodamine B decorated triazole bridged dendrimers were effectively produced up to second generation. The photophysical characteristics of (S)-BINOL cored, rhodamine B decorated dendrimers demonstrated that the fluorescence intensity and light absorption capacity

both increase with dendrimer production. The chiro-optical characteristics similarly demonstrated that the specific rotation rises as dendrimer formation increases, indicating that the dihedral angle at the (S)-BINOL unit widens as the bulkiness of the dendritic wedges grows. In cyclic voltammetry, all dendrimers exhibit quasi-reversible behavior. From the 0th to the 2nd generation of dendrimers, the anticancer activity against human hepatocellular carcinoma cells rises.

REFERENCES

1. Reek J. Valo S. Van Heerbeek R. Kamer P. Van Leeuwen P. *Adv. Catal.* 2006; 49:71–151.
2. Crampton H. Simanek E. *Polym. Int.* 2007; 56:489–496. Doi: 10.1002/pi.2230.
3. Tamali D. A. Reyna L. Svenson S. *Biochem. Soc. Trans.* 2007; 35:61–67. Doi: 10.1042/BST0350061.
4. Svenson S. Tomalia D. A. *Adv. Drug Delivery Rev.* 2005; 57:2106–2129. Doi: 10.1016/j.addr.2005.09.018.
5. Kofoed J. Reymond J. L. *Curr. Opin. Chem. Biol.* 2005; 9:656–664. Doi: 10.1016/j.cbpa.2005.10.013.
6. Scholl M. Kadlecova Z. Klok H.-A. *Prog. Polym. Sci.* 2009; 34:24–61. Doi: 10.1016/j.progpolymsci.2008.09.001.
7. Dvornic P. R. *J. Polym. Sci., Part A: Polym. Chem.* 2006; 44:2755–2773. Doi: 10.1002/pola.21368.
8. Fischer M. Vogtle F. *Angew. Chem., Int. Ed.* 1999;38:884–905. Doi: 10.1002/(SICI)1521-3773(19990401)38:7<884:AID-ANIE884>3.0.CO;2-K.
9. Stadlbauer W. *Sci. Synth.* –324. [Google Scholar]
10. Rajkumar P. Selvam S. Shanmugaiah V. Mathivanan N. *Bioorg. Med. Chem. Lett.* 2007; 15:5270–5273. Doi: 10.1016/j.bmcl.2006.12.071. [PubMed] [CrossRef] [Google Scholar]
11. Thiru Narayanan A. Raja S. Mohanraj G. Rajkumar P. *RSC Adv.* 2014; 4:41778–41783. Doi: 10.1039/C4RA04967E. [CrossRef] [Google Scholar]
12. Anandhan R. Kannan A. Rajakumar P. *Synth. Common.* 2017; 47:671–679. Doi: 10.1080/00397911.2016.1254800. [CrossRef] [Google Scholar]
13. Jayanthi M. Rajakumar P. *Int. j. eng. sci. invention res. dev.* 2016; 3:125–133. [Google Scholar]
14. Zhang K. Zhang C. He Z.-H. Huang J. Du X. Wang L. Wang Q. *ChemBioChem.* 2018; 19:2293–2299. Doi: 10.1002/cbic.201800458. [PubMed] [CrossRef] [Google Scholar]
15. Rajakumar P. Anandhan R. Kalpana V. *Synlett.* 2009; 9:1417–1422. Doi: 10.1055/s-0029-1217170. [CrossRef] [Google Scholar]
16. Ma L. Lee S. J. Lin W. *Macromolecules.* 2002; 35:6178–6184. Doi: 10.1021/ma020283a. [CrossRef] [Google Scholar]

17. Liu G.-H. Fan Q.-H. Yang X.-Q. Chen X.-M. *Arkivoc.* 2003:123. [Google Scholar]